



UNIVERSITY OF LEEDS

This is a repository copy of *Microscopy of nanoparticulate dispersions*.

White Rose Research Online URL for this paper:

<http://eprints.whiterose.ac.uk/89145/>

Version: Accepted Version

---

**Article:**

Brydson, R, Brown, A, Hodges, C et al. (2 more authors) (2015) Microscopy of nanoparticulate dispersions. *Journal of Microscopy*, 260 (3). pp. 238-247. ISSN 0022-2720

<https://doi.org/10.1111/jmi.12290>

---

**Reuse**

Unless indicated otherwise, fulltext items are protected by copyright with all rights reserved. The copyright exception in section 29 of the Copyright, Designs and Patents Act 1988 allows the making of a single copy solely for the purpose of non-commercial research or private study within the limits of fair dealing. The publisher or other rights-holder may allow further reproduction and re-use of this version - refer to the White Rose Research Online record for this item. Where records identify the publisher as the copyright holder, users can verify any specific terms of use on the publisher's website.

**Takedown**

If you consider content in White Rose Research Online to be in breach of UK law, please notify us by emailing [eprints@whiterose.ac.uk](mailto:eprints@whiterose.ac.uk) including the URL of the record and the reason for the withdrawal request.



[eprints@whiterose.ac.uk](mailto:eprints@whiterose.ac.uk)  
<https://eprints.whiterose.ac.uk/>

## Microscopy of Nanoparticulate Dispersions

Rik Brydson<sup>1,2\*</sup>, Andy Brown<sup>1</sup>, Chris Hodges<sup>3</sup>, Patricia Abellan<sup>2</sup> and Nicole Hondow<sup>1</sup>

<sup>1</sup>Institute for Materials Research,  
School of Chemical and Process Engineering,  
University of Leeds,  
Leeds LS2 9JT,  
United Kingdom.

<sup>2</sup> SuperSTEM Laboratory,  
STFC Daresbury Campus,  
Daresbury WA4 4AD,  
United Kingdom

<sup>3</sup> escubed Ltd  
Leeds Innovation Centre  
103 Clarendon Road  
Leeds LS2 9DF,  
United Kingdom

\*corresponding email: [mtlrmb@leeds.ac.uk](mailto:mtlrmb@leeds.ac.uk)

### Summary

We present a critical review of the common methods for determining the dispersion state of nanoparticulate samples particularly in liquid media, including the determination of particle size and morphology; particle size distributions and polydispersity; and equilibrium particle structure and chemistry. We highlight the potential contributions of both scanning probe and electron microscopies in this analysis which is of benefit in understanding nanoparticulate formulations and their behaviour applied across a very wide range of technologies and industry sectors.

## Introduction

Most formulated fine chemical products in foods, home and personal care, healthcare, pharmaceuticals, agrochemicals, catalysts and coatings industries are **complex products** that contain solid, liquid or microcapsule particulates. These are often modified by physical adsorption and/or chemical reaction to increase product stability and enhance the performance of the “active” ingredients. An emerging trend in particulate products is the use of engineered nanoparticles (NPs) which are of intrinsic interest owing to high surface area to volume ratios and the fact that they can exhibit quantum confinement effects. Both these characteristics give rise to the potential ability to display size-dependent functions and properties which are vastly different from that of the bulk form (Hornyak et al., 2008). There has been much recent research focussed on engineered NPs, with a range of proposed applications in biomedicine (as imaging probes for cells and tissues, drug delivery systems and sensors of target molecules), environmental remediation, catalysis, data storage, and lighting technology, as well as within existing fine chemical products.

In the majority of the above applications, NPs are often dispersed within a host medium or matrix, either solid, liquid or gas. A key factor to consider is how a particular NP type may be transformed by this dispersion process. NPs can disperse individually, agglomerate (via weak physical bonds), aggregate (via stronger chemical bonds), sediment out, chemically react (either totally or only partially, e.g. dissolve in a liquid) and even re-precipitate or complex as a second phase (i.e. undergo structural and chemical transformation). In order to correlate, structure and properties, it is therefore vital to determine the following characteristics of the stock and dispersed system: particle sizes and in some cases morphology; particle size distributions and polydispersity; final or equilibrium particle structure and chemistry.

When NPs are dispersed within a solid matrix to form a nanocomposite, information on the NP size and spatial distribution can largely be determined using established volume microscopy techniques. These approaches differ in terms of the field of view (or sample volume) probed and the resolution achievable (Fig. 1) and include: X-ray tomography (volume up to  $\approx$  cubic mm, resolution  $\approx$  1  $\mu$ m or below) (Withers, 2007); serial block face scanning electron microscopy (SBF – SEM) (volume  $\approx$  a few 100 cubic  $\mu$ m, resolution  $\approx$  tens of nm) (Zankel et al., 2009); 3D focused ion beam (FIB)/SEM sectioning (volume  $\approx$  10 cubic  $\mu$ m, resolution  $\approx$  10 nm) (Cantoni & Holzer, 2014); Transmission electron microscopy (TEM) tomography of thin sections (volume  $\approx$  hundreds of cubic nm, resolution  $\approx$  1 nm) (Saghi and Midgley, 2012). Key issues here include: (a) the requirement that the material needs to be unaltered as a result of sample preparation, as well as resistant to radiation damage and contamination during sectioning and/or imaging; (b) the ability to resolve individual NPs; (c) the choice of imaging mode, in that there needs to be sufficient contrast between the NPs and the matrix to allow detection, and furthermore for tomographic reconstruction the signal needs to monotonically increase with increasing thickness. For electron microscopy-based techniques, the latter consideration has led to the use of backscattered imaging and energy dispersive X-ray (EDX) mapping in the SEM, as well as high-angle annular dark field (HAADF) imaging in the Scanning TEM (STEM), EDX or Electron Energy Loss (EEL) spectrum imaging in the STEM and energy filtered imaging in the TEM (EFTEM). The spectroscopic techniques of EDX, EELS and EFTEM are also capable of providing compositional and chemical information.

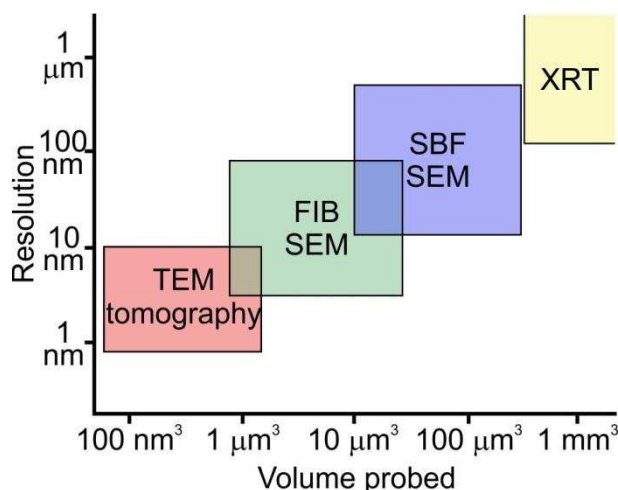


**Fig.1.** Schematic comparing the resolution and volume capabilities of different microscopy techniques that can be used to examine nanoparticles dispersed in a solid matrix. It should be noted all techniques require some level of processing and post data capture, to produce volume reconstructions.

Characterising NP dispersions in solid matrices, particularly where there is a distinct chemical or structural difference between the NPs and the matrix is relatively straightforward and has been employed to study differing types of composites, including heterogeneous catalysts, precipitation-strengthened alloys and nanoparticles distributed within biological materials. For reviews of the relevant X-ray and electron-based tomographic techniques applied to solids, see for example Withers (2007) and Saghi and Midgley (2012).

Characterising NP dispersions in gases is also relatively straightforward as long as the NPs can be faithfully captured onto a substrate suitable for imaging using the appropriate microscopic technique (i.e. without alteration of agglomerate structure or size). This analysis is of use for studying both gas phase nanoparticle formation processes and also environmental science such as NP pollution. Although we do not intend to discuss this area further, Smith et al. describes a method for collecting gas phase nanoparticle dispersion samples with analysis conducted by TEM imaging, EDX spectroscopy and selected area electron diffraction to identify airborne particles that might produce adverse environmental and health effects. This method, minimises any chemical or physical alteration to the particles and the impact of one upon another but still requires the collection of particles onto substrates and will result in the loss of semi-volatile particle components (Smith et al., 2012).

In many situations, such as during chemical product formulation or product delivery processes where particle function rather than structure is of paramount importance, NPs are dispersed within a liquid phase and the characterisation of the resultant NP dispersion then presents considerably more of a challenge than is the case for an all-solid system. Analysis of liquid phase NP dispersions is the main purpose of this present review. More generally, the ability to study such liquid-based systems can provide insight into a variety of crystallisation and dissolution processes involving nanoparticles. In terms of crystallisation, it has enabled investigation of the relevance of concepts such as pre-nucleation clusters, transient amorphous phases, oriented NP attachment and the formation of mesocrystals.

## **General methods for analysing particulate dispersions in liquids**

The distribution of engineered NPs in a simple aqueous suspension is controlled by factors such as ionic strength, pH and temperature of the liquid solution, as well as size and surface chemistry of the particles. In biological and environmental media additional factors need to be considered such as the presence of biomacromolecules, natural organic matter and natural mineral colloids. As a result of this complexity, one has to be careful to probe the distribution of the engineered NPs and not that of other insoluble components of the medium.

Table 1 summarises the major non-microscopy techniques employed to analyse particulate dispersions. Many of these methods may be described as three dimensional “bulk” methods, in contrast to the microscopy-based methods, discussed below, which are often two dimensional in that they image surfaces or provide two dimensional projections of dispersions. Furthermore, these bulk 3D measurements most often measure the hydrated particle size that is influenced by the charge of the particle and the ion concentration in the liquid which determines the thickness of the hydration layer. Thus the term particle size may be technique and application dependent. By far the most commonly used method is dynamic light scattering (DLS) as this assesses large numbers of particles in solution and provides a robust and quantitative measure for narrow particle size distributions. There exist, however, some common problems associated with the majority of the techniques, including DLS. Firstly, relative to microscopy-based approaches, all the methods are indirect and rely on the extraction of nanoparticle sizes via use of some basic assumption to interpret the data (e.g. the presence of spherical particles) or may even employ a more complex data-fitting procedure. As noted above, indirect methods may have inherent difficulties identifying the signal contribution associated with the NPs of interest when dispersed in more complex systems. Secondly, all techniques struggle at very low NP concentrations (where detection is an issue) and also at very high NP concentrations (where signal overlap is an issue); generally each technique possesses an optimal concentration range which may need to be achieved before reliable analysis becomes possible.

As we shall see, concentration can also be a problem for microscopic methods, although increased specimen numbers and specific phase identification with additional, spectroscopic tools are ways of overcoming this.

### **Imaging Liquid Dispersions**

Microscopy techniques can complement bulk nanoparticle dispersion measures such as that achieved by DLS, and are principally used to measure the primary size of NPs but can also give information on agglomerates. By their very definition, nanoparticles lie below the diffraction-limited resolution of conventional light microscopy, leading to the extensive use of scanning probe and electron microscopies. In simple monodisperse systems there is often excellent agreement between DLS and say TEM, and despite the general requirements and conditions for EM (ultra-high vacuum, thin samples etc.), TEM can be used to confirm qualitatively the degree of NP agglomeration suggested by DLS. The aggregates or agglomerates formed by NPs can have complicated 3-D shapes that are not easy to assess by DLS but can be revealed by EM and X-ray tomographic reconstruction provided the specimen preparation adequately preserves the original or native structure (Figure 1).

Overall, imaging nanoparticles in a liquid medium suggests three different potential strategies: (a) image the dispersion in its “wet” state; (b) dry the dispersion and then subsequently image, or; (c) capture/lock-in the dispersion state in some way and image as a

solid. The first option is the most ideal, but can present severe problems as we have a complex multiphase system that can be difficult to control or optimise for imaging purposes. The second option can suffer from potentially severe artefacts induced by drying, principally those caused by the retreating liquid meniscus either disrupting agglomerates, or alternatively forming NP aggregates. In addition, as the liquid evaporates, salt particulates can crystallise out from the solution used to disperse the NPs, complicating identification and analysis of the actual nanoparticles. A further factor may be the collapse of hydrated particle structures when in a vacuum environment. Methodologies for capturing dispersions are outlined in section 4 below.

### Scanning probe microscopy

Scanning Probe Microscopy (SPM), principally Atomic Force Microscopy (AFM) has been used extensively to image dispersions of nanoparticulates, see for example Baalousha & Lead (2013). In all cases, the nanoparticles need to be attached to a suitable substrate (e.g. mica or highly oriented pyrolytic graphite) and there may be the need for some form of prior surface functionalisation of either the nanoparticles and/or the substrate to promote adherence. A general issue for any substrate attachment process is that it may result in a change in the form of the nanoparticle dispersion (i.e. the dispersion may be different to that in the free liquid). Surface attachment is generally more difficult for softer particulates.

Deposition of the nanoparticles onto the substrate can be done by a number of methods: adsorption, i.e. simply suspending the substrate in the dispersion followed by removal; depositing a drop of the dispersion on the substrate, or; ultracentrifugation onto a substrate suspended at the bottom of an Eppendorf tube.

Once the particles are attached onto the substrate, the sample can be imaged either wet, in a liquid cell, or allowed to dry under ambient pressure. In the latter case, it may be important to avoid the drying artefacts already mentioned. Almost any liquid is possible to be used as long as it is transparent to the laser light used to track the AFM probe during its movement. AFM is most often undertaken in tapping mode using either a silicon nitride or silicon tip, the tip radius is typically 10-20 nm (less for specialised tips such as carbon nanotubes). The tip radius governs resolution in terms of the analysis of primary particle size in monodispersed systems, although in principle tip size effects can be deconvoluted from the data. For agglomerated systems the cone angle of the tip is also important as this determines how far the probe can reach into the gaps between primary particles. AFM scanning times can be relatively slow compared to say SEM, although modern instruments can create images in just a few seconds, but this strongly depends on the system being studied.

Besides the tip size and cone angle, the presence of contaminants can limit resolution. The presence of excess surfactants can mask the morphology of underlying nanoparticles or contaminate the tip; one option is to wash the nanoparticles once attached to the substrate, another is to functionalise the tip to avoid pick-up of say long chain surfactants. In some cases it may even be possible to softly scan on top of the contaminant layer before scanning with a larger normal force to image the particles underneath.

For use with nanoparticles, AFM works best with a low concentration of particles thinly dispersed over a very flat substrate (Klapetek et al, 2011). Figure 2 shows a representative AFM image. More complex systems may be analysed, but it is significantly easier for systems that are relatively monodisperse, as in these cases much larger particles cannot

“mask” much smaller ones. If nanoparticles within one sample have significantly different mechanical properties then the AFM response will vary over the scanned area. Usually this is not a problem unless the particles are extremely soft (e.g. hollow polymer shells or micelles), and even these very soft particles may be imaged under carefully controlled conditions. Angular particles can also present problems, particularly if the angularity is sharper than the radius of curvature of the AFM tip. Altering the scan direction and force can help identify any artefacts associated with these systems.

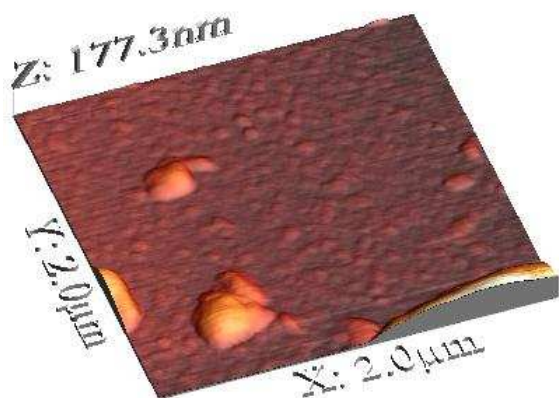


**Fig 2.** AFM image of a set of polymeric nanoparticles adsorbed from liquid onto a flat, hydrophilic glass surface. These 60 – 80 nm particles are quite soft and difficult to image with most other techniques. Note the much larger particle at the front and the agglomerates on the left hand side of the image. The AFM probe allows not only the size but also the softness to be investigated.

A major attraction of AFM is that it can directly measure particle-particle interactions under liquid (i.e. in-situ) by attaching a particle to a suitable probe and using this to investigate the variation in the long and short ranges forces of interaction between the particles as the separation is altered. This works well for individual particles down to 1  $\mu\text{m}$  or so. For nanoparticles, the usual method is to pre-form a substrate coated in a uniform layer of the nanoparticles, and to attach a cluster of nanoparticles to the end of the AFM tip using a micromanipulator and a suitable adhesive if required (Pyrgiotakis et al, 2013). In these cases the exact geometry will vary significantly, but changes introduced in the liquid (salt concentration, pH etc.) will usually significantly change the interaction forces and these may be readily measured and linked to, say, DLS measurements of agglomeration.

### Electron microscopy

A major potential benefit of electron microscopy-based approaches is the possibility to access analytical information on particle composition using for instance EDX, EELS or EFTEM, or crystallography using say electron diffraction in the TEM.

In principle, environmental scanning electron microscopy (ESEM) permits the imaging of wet samples via accommodation of a low pressure of a gas around the (cooled) sample, which in the case of water allows hydrated samples to be imaged in their native state. Colloidal dispersions have been investigated using ESEM, but great care is required to maintain the sample hydrated during the instrument pump down cycle and the sample conditions

(temperature and water vapour pressure) need to be well controlled. In reality, resolution limitations have meant that only relatively large particles have been investigated and furthermore, most studies have focused on aggregation and drying rather than imaging dispersions in the pristine state (Stokes, 2008).

Imaging of NP-bearing solutions in a transferrable environmental/liquid cell within the vacuum system of an electron microscope is also being developed but this can be costly and is currently a relatively low resolution approach. Nonetheless the prospect of real-time analysis of NP agglomeration in suspensions viewed by electron microscopy (both SEM and TEM) of liquid cells is very realistic and exciting. However, as is the case for ESEM, the effect of the electron beam on the sample, the liquid and in this case the membrane of the liquid cell must be understood before robust comparison to complex samples can be made.

#### Liquid cells for electron microscopy

Commercial (SEM and TEM) liquid cell sample holders or specialised electron microscopes with inbuilt liquid sample capacity (e.g. the JEOL Clairscope - an inverted SEM) are available for both SEM and TEM (Fig. 3). All designs incorporate a membrane that prevents evaporation of the liquid sample in the microscope vacuum. This membrane is most often composed of thin (typically 10-50 nm) silicon nitride which can be functionalised with surfactants or plasma-treated to provide either a positively or negatively charged surface, or (depending on the liquid and nanoparticle type) either a hydrophobic or hydrophilic surface. Functionalization of the membrane may assist nanoparticle attachment to the membrane which aids the imaging process. However, major issues associated with the use of a membrane include: alterations to the particle dispersion arising as a result of the membrane attachment process itself (see above), charging of the membrane under the electron beam, and secondary electron production in the membrane which could result in localized or enhanced radiolytic damage to either the NPs or the liquid close to the membrane.

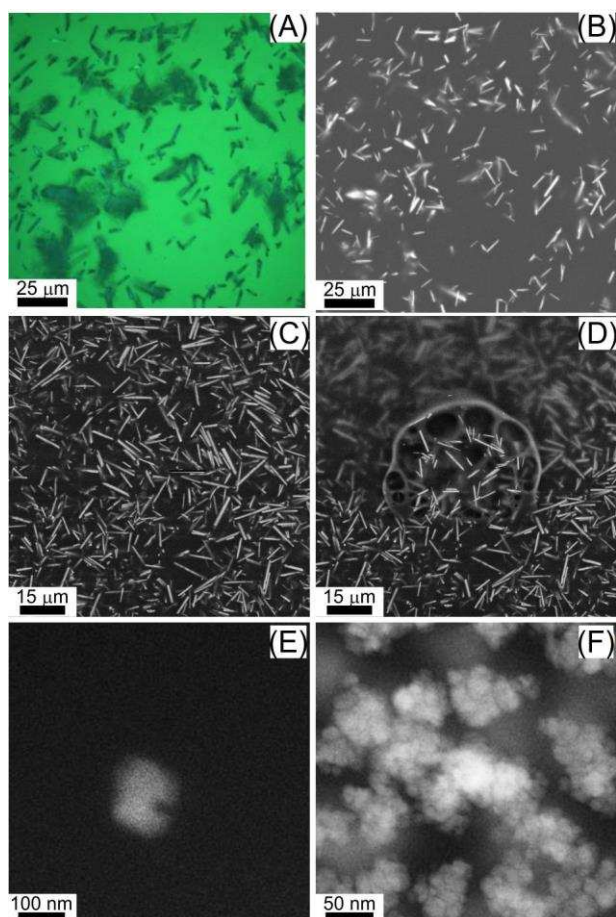


**Fig. 3.** Imaging nanoparticles dispersed in liquids using electron microscopy. Correlative reflected light (a) and scanning electron (b) imaging of ZnO nanorods using an atmospheric SEM. ZnO nanorods further examined using a liquid cell in the SEM (c), image alteration after repeated acquisition, indicating interaction between the irradiated fluid and membrane which becomes damaged after several repeated images (d). ZnO nanoparticles examined using a TEM liquid cell holder and imaged in HAADF STEM mode (e), where flocculates of zinc oxide or salts are produced when the electron beam is focused on a region at high magnification for 10 seconds (f). It should be noted that flocculation, as seen in (f), is observed in two distinct planes (two distinct focal planes) corresponding to the top and bottom membranes. This could be due to either (or possibly both) that the membrane surfaces are preferential nucleation sites (the energy barrier for heterogeneous nucleation is lower than for homogeneous nucleation in the bulk of the solution) or to an enhanced presence of secondary electrons at the membrane surface due to their production as the electron beam interacts with the membrane itself.

A further concern is radiolysis of the liquid itself. The chemical effect of ionizing radiation on liquids/liquid media has been a major topic of study for many years particularly in relation to cancer radiotherapy, atmospheric science, remediation of waste-water, food preservation/treatment, sterilization of pharmaceuticals, synthesis and nuclear energy production. A distinct difference with electron microscopy is that electron dose rates (and hence total electron doses) are many orders of magnitude higher than those generated by other common radiation sources. The absorbed dose rate is strictly measured in Grays per second (note a Gray (Gy) is 1 Joule of energy deposited per kg of matter or per unit volume), typically for 100 keV electrons and a typical organic material then an electron fluence of 1 electron/Å<sup>2</sup> or ca.  $1.6 \times 10^{-3}$  C/cm<sup>2</sup> is equivalent to a total absorbed dose of 4 MGy,

and is in many cases sufficient to initiate degradation of the material; other (non-organic) materials may be somewhat more resistant to damage. Dose rate is often also very important as in addition to damage, there are most often reverse processes in operation which can “heal” the results of damage. Radiolysis of aqueous liquid systems results in the production of molecular and radical products such as hydrated electrons, H<sup>•</sup> atoms, OH<sup>•</sup> radicals, hydrogen and oxygen, which can lead to beam induced charging, gas bubble formation, pH changes, increases in the ionic strength of the solution and changes in NP chemistry. These can all severely affect the dispersion state and chemistry of the nanoparticles potentially causing heterogeneous nucleation of particles on the membrane, particle agglomeration (including self-organisation of NPs on the membrane), aggregation, etching and growth of the nanoparticles, or even NP dissolution. Furthermore, mass transport of species produced by radiolysis outside the irradiated volume can also occur. Any of these events can have severe implications for studying dynamic processes (e.g. crystallisation or dissolution) within a dispersion or solution using liquid cell electron microscopy, as any changes in pH, particle charge or concentration including supersaturation can severely modify behaviour. Abellan et al. (2014) discuss factors influencing quantitative imaging in liquid cells and Schneider et al. (2014) have produced a predictive model to calculate the radiolysis effects in water under a given set of microscope beam conditions. Typically dose rates have to be kept at or below MGy per second to avoid unwanted alteration (Woehl et al., 2013), and consideration should be given to the effects of different imaging modes, i.e. global irradiation in TEM versus local irradiation in STEM.

On a cautionary note, it should be mentioned that there are already many observations in the literature using both SEM and TEM liquid cells which would appear to be almost entirely due to electron beam induced effects in the liquid. With careful work, many of these complex radiolytic effects in the liquid are now being understood and mitigation strategies developed. Key findings include: the minimisation of the dose rate for reliable results; observation by STEM seems advantageous relative to TEM; non-polar liquids are less susceptible to damage than polar liquids; and scavengers can be added to liquids to mop up reactive radical species created during radiolysis. Taking these findings into consideration, representative imaging of nanoparticles dispersed in liquids using electron microscopy is becoming an exciting prospect.

### **“Capturing Dispersions”– drying and freezing**

An alternative to imaging the liquid directly is to try and capture the nanoparticle dispersion state in its solid form and image using conventional microscopies. The key issue here is to examine the dispersion in its native state, i.e. without alteration during the sample preparation procedure. As discussed for AFM, the most basic approach is to either drop-cast; ultracentrifuge or simply adsorb the dispersion on a sample support substrate and allow it to dry at ambient pressure. However, as discussed and particularly for the case of drop-casting, drying can induce NP agglomeration or even breakup of agglomerates, negating quantitative sizing. Furthermore drying can lead to precipitation of soluble salts within the liquid medium which can severely complicate analysis. A major issue with electron microscopy (relative to AFM) is the fact that the dried dispersion is imaged under vacuum in the electron microscope which may lead to the removal of water intrinsic to the nanoparticulate structure and hence lead to collapse of the particles. This may explain why particle volumes measured by TEM have been noted to be smaller than those derived by AFM (Posfai et al., 1998).

Alternatively it is possible to prepare samples by rapid freezing of the dispersion with sufficient speed to ensure the aqueous phase vitrifies with no significant redistribution of suspended material. There are two potential methods to achieve this: high pressure freezing (HPF) of a large droplet (a few microlitres) of the dispersion between two aluminium planchettes; or plunge freezing (PF) a much smaller quantity of the blotted dispersion on a holey carbon TEM grid by rapid immersion in liquid nitrogen cooled liquid ethane.

In the former case, samples up to a thickness of 200  $\mu\text{m}$  can be frozen, freeze fractured and then imaged in an electron microscope with a cryostage. Cryogenic methods of sample preparation have long been used in cell biology and more recently for imaging of nanoemulsions (Klanget al. 2012). It is also possible to probe the full three dimensional dispersion by serial sectioning of cryo-prepared specimen blocks by cryo-FIB; for example, Holzer et al. (2007) have quantitatively analysed particle structures in cement suspensions. Alternatively, HPF of a small amount of suspension in a copper tube could be undertaken and then cryosectioned in a cryo-ultramicrotome. The thin frozen section and hence the frozen dispersed state could be imaged using a TEM cryoholder and cryo-electron microscopy of vitrified sections (CEMOVIS). Fundamentally though, the primary challenge is of artefact-free sample preparation and this remains because both freeze fracture and CEMOVIS could lead to distortion of dispersed NP aggregates. Other non-cryo specimen preparation methods to capture dispersion include using a gel such as agarose to solidify an aqueous suspension of nanoparticles (Saville et al. 2013). The resulting gel can then be resin infiltrated, embedded and sectioned for TEM analysis and may not suffer the same sectioning distortion if the resin hardness is carefully selected.

In the latter case of plunge freezing, in which a drop of NP suspension is placed onto a standard TEM support film, blotted and rapidly frozen may also lead to some flattening of the sample and any NP aggregates therein. However, the resultant plunge frozen sample could be directly imaged (potentially following a negative stain – i.e. staining of the fluid phase rather than the nanoparticles) in a cryo-TEM even using cryotomography for three dimensional information. Cryo-TEM and –tomography has been used to investigate the initial stages of template-controlled  $\text{CaCO}_3$  formation, directly imaging prenucleation clusters and the amorphous nanoparticles that are formed by the aggregation of the clusters (Pouget et al., 2009). Alternatively, if the suspension contains pre-formed nanoparticles, the frozen section could be allowed to warm under vacuum (vacuum sublimation) as this improves image contrast and has been shown to largely preserve agglomerate structure because there is insufficient thermal energy for significant growth of crystalline ice and redistribution of particles before the solidified aqueous phase sublimates. This approach has recently been used to measure and quantify the dispersion of ZnO and polymer coated CdTe/ZnS NPs in cell delivery media to overcome inconsistent particle measurement by DLS (Fig. 4; Hondow et al., 2012; Wallace et al., 2012).

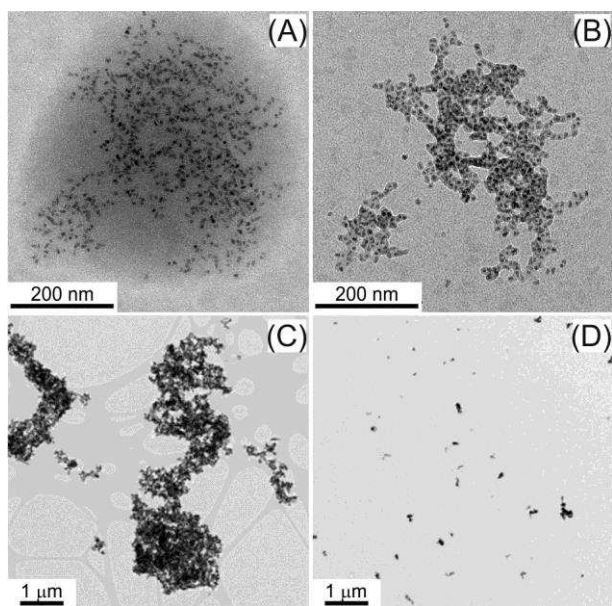


**Fig. 4.** Cryo-TEM capturing NP dispersions using rapid freezing. (a) TEM image of an agglomerate of quantum dots dispersed in water imaged under cryo conditions and (b) after warming in vacuum to a temperature where the surrounding ice has devitrified and sublimated. TEM image of ZnO nanoparticles prepared by conventional drop-casting (c) where nanoparticles can dry together and (d) after preparation involving freezing followed by warming under vacuum, showing the ZnO nanoparticle agglomerates that were originally present in the suspension. (a) and (b) reproduced from N. Hondow et al. 2012, *J. Nanopart. Res.*, 14:977, with kind permission from Springer Science and Business Media.(c) and (d) reproduced from R. Wallace et al. 2012, *J. Phys. Conf. Ser.* 371, 012080.

## Conclusions

Scanning probe and electron microscopies can be used to quantify and measure NP dispersion, however care must be taken to ensure sample preparation is appropriate and representative. Microscopy techniques provide additional information to bulk methods where NP concentrations or dispersion media conditions are challenging or where individual nanoparticle information is required. Furthermore, using microscopy approaches to assess nanoparticle dispersion provides direct imaging to determine primary particle size and the potential to probe structure and chemistry. Scanning probe microscopy of NP dispersion in liquids requires relatively dilute suspensions but can be used to directly measure particle to particle interactions. There are significant prospects for the use of liquid cells to directly image nanoparticle suspensions and identify agglomerate status by electron microscopy, however the effects of imaging conditions on the suspending fluid (e.g. agglomeration or alteration induced by radiolysis) will need to be fully investigated for each individual system. Rapid freezing protocols therefore currently dominate the specimen preparation methods for the analysis of agglomeration in NP suspensions by electron microscopy. Ultimately, validation against bulk measures is recommended where possible, and in particular as all techniques provide both advantages and limitations, a combination of analysis techniques will be most robust.

## Acknowledgements

We would like to thank Pippa Hawes (The Pirbright Institute) for helpful discussions. We would like to acknowledge the help and work of James Cattle (University of Leeds), Ian

Morrison (University of York) and Peter O'Toole (University of York) on the atmospheric SEM experiments (conducted on the JEOL JASM-6200 ClairScope in the Department of Biology, University of York); James Cattle (University of Leeds) on liquid cell SEM experiments (conducted using QuantomiX QX-capsules at the Leeds Electron Microscopy and Spectroscopy Centre); and Rachel Wallace (University of Leeds), Andreas Verch (University of York) and Roland Kröger (University of York) on liquid cell TEM experiments (conducted using a Protochips Poseidon holder at the York JEOL Nanocentre).

## References

Abellan, P., Woehl, T.J., Parent, L.R., Browning, N.D., Evans, J.E. & Arslan, I. (2014) Factors influencing quantitative liquid (scanning) transmission electron microscopy. *Chem. Commun.* **50**, 4873-4880.

Baalousha, M. & Lead, J.R. (2013) Characterization of natural and manufactured nanoparticles by atomic force microscopy: Effect of analysis mode, environment and sample preparation. *Colloid. Surface A* **419**, 238-247.

Cantoni, M. & Holzer, L. (2014) Advances in 3D focused ion beam tomography. *MRS Bull.* **39**, 354-360.

Holzer, L., Gasser, Ph., Kaech, A., Wegmann, M., Zingg, A., Wepf, R. & Muench, B. (2007) Cryo-FIB-nanotomography for quantitative analysis of particle structures in cement suspensions. *J. Microsc.* **227**, 216-228.

Hondow, N., Brydson, R., Wang, P., Holton, M. D., Brown, M. R., Rees, P., Summers, H. D. & Brown, A. (2012) Quantitative characterization of nanoparticle agglomeration within biological media. *J. Nanopart. Res.* **14**, 977.

Hoo, C.M., Starostin, N., West, P. & Mecartney, M.L. (2008) A comparison of atomic force microscopy (AFM) and dynamic light scattering (DLS) methods to characterize nanoparticle size distributions. *J. Nanopart. Res.* **10**, 89-96.

Hornyak, G. L., Tibbals, H. F., Dutta, J. & Moore, J.J. (2008) *Introduction to Nanoscience and Nanotechnology*, Taylor and Francis CRC Press, Boca Raton, Florida.

Klang, V., Matsko, N.B., Valenta, C. & Hofer, F. (2012) Electron microscopy of nanoemulsions: An essential tool for characterisation and stability assessment. *Micron* **43**, 85-103.

Klapetek, P., Valtr, M., Nečas, D., Salyk, O. & Dzik, P. (2011) Atomic force microscopy analysis of nanoparticles in non-ideal conditions. *Nanoscale Res. Lett.* **6**, 514.

Posfai, M. , Xu, H., Anderson, J.R., & Buseck, P.R. (1998) Wet and dry sizes of atmospheric aerosol particles: An AFM-TEM study. *Geophys. Res. Lett.* **25**, 1907-1910.

Pouget, E.M., Bomans, P.H.H., Goos, J.A.C.M., Frederik, P.M., de With, G. & Sommerdijk, N.A.J.M. (2009) The initial stages of template-controlled CaCO<sub>3</sub> formation revealed by cryo-TEM. *Science* **323**, 1455-1458.

Pyrgiotakis, G., Blattmann, C.O., Pratsinis, S. & Demokritou, P. (2013) Nanoparticle-nanoparticle interactions in biological media by atomic force microscopy. *Langmuir* **29**, 11385-11395.

Saghi, Z. & Midgley, P. A. (2012) Electron Tomography in the (S)TEM: From Nanoscale Morphological Analysis to 3D Atomic Imaging. *Annu. Rev. Mater. Res.* **42**, 59–79.

Saville, S.L., Woodward, R.C., House, M.J., Tokarev, A., Hammers, J., Qi, B., Shaw, J., Saunders, M., Varsani, R.R., St Pierre, T.G. & Mefford, O.T. (2013) The effect of magnetically induced linear aggregates on proton transverse relaxation rates of aqueous suspensions of polymer coated magnetic nanoparticles. *Nanoscale* **5**, 2152-2163.

Schneider, N.M, Norton, M.M., Mendel, B.J., Grogan, J.M., Ross, F.M. & Bau, H.H. (2014) Electron–Water Interactions and Implications for Liquid Cell Electron Microscopy. *J. Phys. Chem. C* **118**, 22373-22382.

Smith, S., Ward, M., Lin, R., Brydson, R., Dall'Osto, M. & Harrison, R.M. (2012) Comparative study of single particle characterisation by Transmission Electron Microscopy and time-of-flight aerosol mass spectrometry in the London atmosphere. *Atmos. Environ.* **62**, 400-407.

Stokes D.J. (2008) Principles and Practice of Variable Pressure/Environmental Scanning Electron Microscopy (VP-SEM), John Wiley and Sons, UK.

Wallace, R., Brown, A.P., Brydson, R., Milne, S.J., Hondow, N. & Wang, P. (2012) Characterisation of ZnO nanoparticle suspensions for toxicological applications. *J. Phys. Conf. Ser.* **371**, 012080.

Withers, P.J. (2007) X-ray Nanotomography, *Mater. Today* **10**, 26-34.

Woehl, T.J., Jungjohann, K.L., Evans, J.E., Arslan, I., Ristenpart, W.D. & Browning, N.D. (2013) Experimental procedures to mitigate electron beam induced artifacts during in-situ fluid imaging of nanomaterials. *Ultramicroscopy* **127**, 53-63.

Zankel, A., Kraus, B., Poelt, P., Schaffer, M. & Ingolic, E. (2009) Ultramicrotomy in the ESEM, a versatile method for materials and life sciences. *J. Microsc.* **233**, 140-148.

**Table I. Non-microscopy techniques to analyse particulate dispersions.**

Technique	Measurement Method	Output	Advantages	Disadvantages
Dynamic Light Scattering (DLS)  Also known as Photon Correlation Spectroscopy (PCS)	Time-dependent variation in Rayleigh scattering of coherent light by NPs undergoing Brownian motion. From this variation it is possible to estimate diffusion coefficients.	Infer a hydrodynamic radius from diffusion co-efficient. <ul style="list-style-type: none"> <li>Applicable to size ranges between 1 nm and ~ 6000 nm.</li> </ul>	<ul style="list-style-type: none"> <li>Very common method to assess large numbers of particles in dispersion.</li> <li>Provides a robust and quantitative measure for narrow particle size distributions.</li> </ul>	<ul style="list-style-type: none"> <li>Assumes spherical particle shape.</li> <li>Not possible to distinguish between different types of NPs</li> <li>Becomes significantly less reliable for the measurement of large particle size dispersity (because of the sixth power dependence of light scattering intensity on the sizes of the scattering particles).</li> <li>Accuracy is also reliant on knowing the refractive index of the NPs and the viscosity and refractive index of the dispersant.</li> <li>Sensitivity is related to the laser power.</li> <li>Can be ineffective at high concentrations due to multiple scattering and at low concentrations if there is not enough signal.</li> </ul>
	Berne, B. J. & Pecora, R. (2000) <i>Dynamic Light Scattering with Applications to Chemistry, Biology, and Physics</i> . Dover Publications Inc.: New York.			
Nanoparticle Tracking Analysis (NTA)	Direct visualisation and tracking of the movement of NPs and agglomerates over time to measure diffusion coefficients of suspended particles.	Infer a hydrodynamic radius from diffusion co-efficient. <ul style="list-style-type: none"> <li>Applicable size ranges are dependent upon particle composition, but are generally 10 nm to 1000 nm.</li> </ul>	<ul style="list-style-type: none"> <li>Directly provides a number concentration of particles; can then back calculate via dilution factor to real sample.</li> <li>Some (but not all) particles of different composition can be distinguished due to differences in scattering intensity.</li> <li>Sensitive to different sizes in polydisperse systems and to different shaped particles.</li> </ul>	<ul style="list-style-type: none"> <li>Dilution to <math>10^7 - 10^9</math> particles/mL needed.</li> <li>Comparable limitations to DLS in terms of low concentrations (~1 mg/L) and the assumption of a spherical NP morphology.</li> <li>Normally requires narrow range of RI and viscosity.</li> <li>Not as reproducible as DLS.</li> </ul>
	Filipe, V., Hawe, A. & Jiskoot, W. (2010) Critical evaluation of nanoparticle tracking analysis (NTA) by NanoSight for the measurement of nanoparticles and protein aggregates. <i>Pharm. Res.</i> , <b>27</b> , 796-810.			
Field Flow Fractionation (FFF)	Different particle mobilities in a separating field (e.g. gravitational, magnetic, electrical, thermal, centrifugal) applied to a dispersion which is pumped through a long and narrow channel.	Physical separation technique of injected masses in the ng – µg range. Detection follows separation and is either on-line (e.g. UV-Vis, ICP-MS, etc) or off-line (following collection, e.g. EM). Particle-mass based size distributions can be determined for homogeneous particles of known composition or stoichiometry. <ul style="list-style-type: none"> <li>Size ranges separated 1 nm to several µm's.</li> </ul>	<ul style="list-style-type: none"> <li>FFF can be coupled with detectors to obtain complementary data, with numerous types of FFF separation (e.g. flow, sedimentation, etc) combined with various detectors (UV-visible spectroscopy, ICP-MS, ICP-AES, etc) in order to provide analysis opportunities.</li> </ul>	<ul style="list-style-type: none"> <li>Dilution or pre-concentration commonly required.</li> <li>Limited range of applicable concentrations.</li> <li>Often not applicable to particles or agglomerates/aggregates &gt; 1 µm.</li> <li>Results often remain non-quantitative for particles of unknown or variable composition or stoichiometry.</li> </ul>
	von der Kammer, F., Legros, S. Larsen, E.H., Loeschner, K & Hofmann, T. (2011) Separation and characterization of nanoparticles in complex food and environmental samples by filed-flow fractionation. <i>Trend. Anal. Chem.</i> , <b>30</b> , 425-436.			

**Table I. cont...**

<b>Technique</b>	<b>Measurement Method</b>	<b>Output</b>	<b>Advantages</b>	<b>Disadvantages</b>
Disc Centrifuge	Separates NP dispersions on a plate via centrifugal sedimentation and measures the distribution by changes in light intensity measured through the disc.	Can give results based on volume fractions and be used to monitor the rate of sedimentation. <ul style="list-style-type: none"> <li>Applicable to sizes ~ 5 nm to 10's of <math>\mu\text{m}</math>'s.</li> </ul>	<ul style="list-style-type: none"> <li>Can detect bimodal particle size distributions.</li> <li>Fine sensitivity; can separate similar particle sizes.</li> </ul>	<ul style="list-style-type: none"> <li>Can underestimate particle diameters, especially of particles with organic coatings (change in effective density).</li> <li>Potential problems with particles which do not sediment.</li> <li>Time-intensive.</li> </ul>
	Mahl, D., Diendorf, J., Meyer-Zaika, W. & Epple, M. (2011) Possibilities and limitations of different analytical methods for the size distribution of a bimodal dispersion of metallic nanoparticles. <i>Colloids Surf. A</i> , <b>377</b> , 386-392.			
Coulter Counter	Employs an electric field to draw NPs through channels and measure the impedance change as the liquid electrolyte is displaced which is proportional to the particle volume.	Produces a plot of current versus time containing a string of current pulses, in which the height of pulse can be related to particle size, width to charge and frequency to concentration. Polarisation intensity differential scattering can be used to distinguish between large and small particles. <ul style="list-style-type: none"> <li>Detected size range is dependent upon the channel size, but potentially 3 nm (but more conventionally 0.4 <math>\mu\text{m}</math>) to 1000's of <math>\mu\text{m}</math>'s.</li> </ul>	<ul style="list-style-type: none"> <li>Size measurement is dependent upon the channel size; the use and development of smaller channels enables the measurement of smaller particles.</li> <li>The particle concentration can be determined.</li> </ul>	<ul style="list-style-type: none"> <li>Operation limited to favourable conditions, with applicability to analysis of NP dispersion in complex media yet to be determined.</li> <li>Smaller and more robust channels are required. Current channels often suffer from poor reproducibility or limited lifetimes.</li> </ul>
	Henriquez, R.R., Ito, T., Sun, L. & Crooks, R.M. (2004) The resurgence of Coulter counting for analysing nanoscale objects. <i>Analyst</i> , <b>129</b> , 478-482.			
Small angle X-ray scattering (SAXS)  Also small angle neutron scattering (SANS)	Fit and model low angle X-ray scattering data.  Often conducted at a synchrotron to achieve data with a sufficiently adequate signal to noise ratio.	Particle size, shape and polydispersity. Can potentially infer aggregate state (with appropriate fittings to data). <ul style="list-style-type: none"> <li>Applicable to sizes as low as 0.8 nm.</li> </ul>	<ul style="list-style-type: none"> <li>Wet cell and also dry powder.</li> <li>Representative measure of the bulk.</li> </ul>	<ul style="list-style-type: none"> <li>Sensitive to the 6<sup>th</sup> power of the particle diameter (<math>d^6</math>) which means large particles dominate the signal.</li> <li>Limited by the need to fit and model scattering data.</li> <li>Scattering of NP dispersions in biological or environmental media can be dominated by the liquid (and other components in the medium), creating issues for measurement of very small (&lt; 5 nm) NP sizes and dilute concentrations.</li> <li>Poor temporal limit, requiring the dispersion to be stable for the analysis period.</li> </ul>
	McKenzie, L.C., Haben, P.M., Kevan, S.D. & Hutchison, J.E. (2010) Determining nanoparticle size in real time by small-angle X-ray scattering in a microscale flow system. <i>J. Phys. Chem. C</i> , <b>114</b> , 22055-22063.			
X-ray Diffraction (XRD)	Debye-Scherrer broadening of XRD peaks.	Volume-averaged crystallite size (which may or may not be equivalent to particle size). <ul style="list-style-type: none"> <li>Applicable to a sizes ~ 30 nm to 100's of <math>\mu\text{m}</math>'s.</li> </ul>	<ul style="list-style-type: none"> <li>Wet cell and also dry powder.</li> <li>Representative measure of the bulk.</li> </ul>	<ul style="list-style-type: none"> <li>Can be affected by strain in particles; in principle can separate the two with a Williamson-Hall type plot.</li> <li>Less reliable for crystallite sizes &lt; 5nm where dispersions can often appear "X-ray amorphous".</li> <li>Assumes spherical particle shape.</li> <li>Wet cell requires a stable dispersion for the analysis period.</li> </ul>
	Cullity B.D. and Stock S.R. (2001), <i>Elements of X-Ray Diffraction</i> , 3rd Ed., Prentice-Hall Inc.: New Jersey.			